JOURNAL OF SOLID STATE CHEMISTRY 32, 269–277 (1980)

Solid-State Electrochemical Studies of the Mixed Conductor $Cu_xMo_6S_{8-y}$. II: Equilibrium Partial Thermodynamic Properties

G. J. DUDLEY,* K. Y. CHEUNG, AND B. C. H. STEELE

Wolfson Unit for Solid-State Ionics, Department of Metallurgy and Materials Science, Imperial College of Science and Technology, Prince Consort Road, London, SW7 2AZ United Kingdom

Received January 10, 1979; in final form May 11, 1979

The equilibrium emf of the cell

$$Pt/Cu/\text{copper electrolyte}/Cu_xMo_6S_{7.59}/Pt$$

has been measured as a function of x and temperature. The resulting values of copper chemical potential, partial enthalpy, and partial entropy are compared with values calculated on the basis of a simple model which takes into account the distribution of copper between two types of site as well as the electronic configuration. There is a broad correspondence between experiment and theory, indicating that the configurational terms are the most important in determining the changes in partial quantities with composition, but more sophisticated treatments would be required to explain the detailed behavior.

Introduction

In recent years there has been a growing interest in compounds of the general formula $M_xMo_6S_8$ because of their electronic superconducting properties. In the accompanying paper (*1*) we have confirmed earlier indications that $Cu_xMo_6S_8$ is a good copper ion conductor, as well as a metallic electronic conductor. Since it also exhibits a large range of stoichiometry it satisfies most of the criteria for a solid solution electrode (SSE) material (*2*). A very important consideration in the use of such materials in batteries is the variation of the open circuit cell emf with state of change. This is determined by the sum of the variations in the chemical potential of the mobile species at each electrode as the metal content is changed. If one of the electrodes has an invariant chemical potential of metal, such as an electrode consisting of the metal itself, then changes in the metal chemical potential in a single SSE material can be followed by means of a series of coulometric titrations. Such measurements have been made on a number of SSE materials such as $K_{1+x}Fe_{11}O_{17}$ (*3*), $Li_{3-x}Sb$ (*4*), and Li_xTiS_2 (*5*).

In contrast to "classical" dilute defect conductors typified by the alkali halides, superionic conductors have very large carrier concentrations and a significant proportion of available sites for the mobile ions are occupied. Therefore when the metal content of a SSE material is changed, it is highly unlikely that the system will behave as a thermodynamically ideal solid solution. For example, Fromhold (*6*) shows that the

* To whom correspondence should be addressed. Present address: Berec Group Ltd., Advanced Projects Group, 18, Nuffield Way, Ashville Trading Estate, Abingdon, Oxon, OX14 1TG, United Kingdom.

0022-4596/80/060269-09$02.00/0

statistical treatment of defects in crystals gives Fermi–Dirac-type results when each site can only accommodate one particle. Armand (*7*) has applied these considerations to SSE materials, especially the layer compounds, and accounted semiquantitatively for several published emf–composition curves by considering the variations with composition of the configurational entropy of the mobile ions and electrons. Furthermore, two phase regions could be explained if variations in an internal energy term, the "intercalation pressure," was considered which represents the energy required by the ions to open up the layers.

The subject of this work, $Cu_xMo_6S_8$, is a three-dimensional ionic conductor and because considerable structural information is already available it was of interest to extend this treatment to this class of compound, which may become important in the development of solid-state batteries.

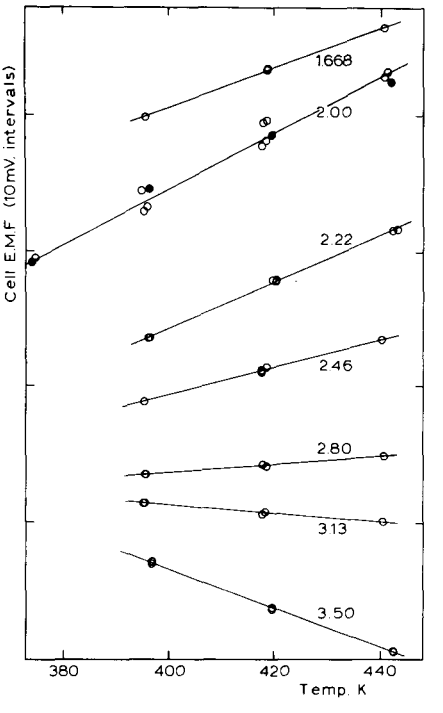

FIG. 1. Cell emf as a function of temperature at different compositions. (The emf axis zero is different for each composition but the scale is the same.) Solid circles at $x = 2.00$ indicate results after composition had been cycled.

Thermodynamics of SSE Materials

Experimental

The equilibrium cell emf data were obtained as a byproduct of the study of transport properties of $Cu_xMo_6S_8$. Details of the cell used and preparation of materials are published in the accompanying paper (*1*). Since the ionic probes contained vacuum-deposited copper metal as the reference material, the voltage measured between ionic and electronic probes in the absence of applied current, and after equilibrium had been obtained, corresponded to that of the cell

$$Pt/Cu_xMo_6S_8/Cu\ \text{electrolyte}/Cu/Pt$$

and allowed measurement of the formal copper metal activity in the sample at each composition and temperature. Figure 1 shows the cell emf as a function of temperature for selected x values. (The origin of the emf axis has been changed for each x value but the scale is constant.) At each composition the temperature was cycled at least once and very good reproducibility in the emf values was obtained, allowing partial enthalpies and entropies to be calculated with reasonable precision despite the small range of temperatures employed. Figure 2 (open circles) shows the cell emf or copper metal activity as a function of x at 400°K. These values were obtained by interpolation of emf–temperature data such as those in Fig. 1. The composition was cycled twice and emf values recorded in each cycle agreed to within 1.5 mV. An earlier coulometric titration cell had given less reliable data, but extended to lower x values where the rate of equilibration was too slow to be covered by the bar assembly. It made use of a simple arrangement of thin pellets with working and

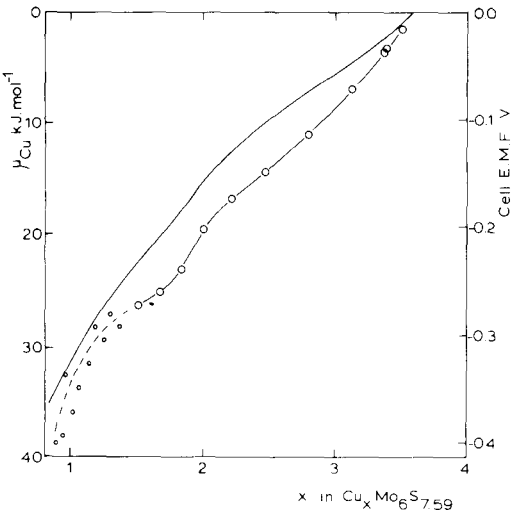

FIG. 2. Chemical potential of copper or cell emf as a function of composition at 400°K. Large open circles: bar experiment; small open circles: pellet experiment; solid line: theoretical model.

reference electrodes. The data from this are shown by the small circles in Fig. 2.

Meaning of the Cell emf

Consider the cell

$$Pt/M/M^+ \text{ electrolyte}/M^+ \text{ SSE}/Pt,$$

where M is a monovalent metal and M^+SSE a solid solution electrode with mobile M^+ and electrons (or holes). It is a concentration cell in metal M and the open circuit emf E is thus given by

$$E = -\Delta\mu_M/F,$$

where $\Delta\mu_M$ is the difference in metal chemical potential between the SSE and the metal itself. From the Gibbs–Helmholtz equation it is possible to split $\Delta\mu_M$ into partial molar entropy ($\Delta\bar{S}_M$) and partial molar enthalpy ($\Delta\bar{H}_M$) terms from a knowledge of the variation of cell emf with temperature at constant pressure (*8*):

$$\Delta\bar{S}_M = F\left[\frac{dE}{dT}\right]_P, \quad \Delta\bar{H}_M = F\left\{T\left[\frac{dE}{dT}\right]_P - E\right\}.$$

General Configurational Entropy Model

Consider a unit cell of the SSE material that contains several types of site for the mobile ions. There are g_1 crystallographically equivalent sites with energy u_1 containing n_1 ions, g_2 sites of energy u_2 containing n_2 ions, and so on. The number of ways of arranging n_1 ions among g_1 sites is $g_1!/n_1!(g_1-n_1)!$ Taking into account all occupied levels, the total number of arrangements ω with a given set of n_j values is

$$\omega = \prod_j g_j!/[n_j!(g_j-n_j)!]. \tag{1}$$

If N is the total number of ions per unit cell and U their total energy then one has

$$\sum_j n_j = N, \tag{2}$$

$$\sum_j n_j u_j = U. \tag{3}$$

Since other arrangements (l) with different n_j values, but the same values of N and U, are possible the total number of distinguishable arrangements (Ω) can be represented by

$$\Omega = \sum_l \prod_j (g_j!/[n_{jl}!(g_j-n_{jl})!]). \tag{4}$$

By conventional statistical arguments (see Appendix) one finds that Ω can be approximated by the largest terms in the summation, containing the most probable values of n_j, denoted n_j^* and given by

$$n_j^* = g_j/(\exp[(u_j-\mu)/kT]+1), \tag{5}$$

where μ is the chemical potential of the ion. This is recognizable as the Fermi–Dirac distribution and appears because each lattice site can only contain one ion. The total entropy and internal energy of the system are given by

$$S = k\sum_j [g_j \ln g_j - n_j^* \ln n_j^* - (g_j-n_j^*)\ln(g_j-n_j^*)], \tag{6}$$

$$U = \sum_j n_j^* u_j. \tag{7}$$

The experimentally measured values are, however, partial molar quantities given by

$$\bar{S} = dS/dN, \tag{8}$$

$$\bar{H} = dH/dN \sim dU/dN. \tag{9}$$

The approximation in Eq. (9) is reasonable since the $P\bar{V}$ contribution due to changes in lattice parameters with stoichiometry of the SSE is expected to be very small. $\bar{S}$ and $\bar{U}$ were computed for pairs of close values of N and the differentiation carried out by finite differences. This allows energy level models of any complexity to be treated.

Provided that the electrons occupy narrow bands they can be considered in the same way as the ions and the resulting quantities added to obtain the partial molar quantities associated with the neutral metal. As an example, Fig. 4 shows the site occupancy (N) and partial thermodynamic quantities for a model in which there are two energy levels each capable of containing two ions (i.e., $g_1 = g_2 = 2$). Results are shown for two values of the energy difference between these levels, namely, 13,302 J mole^{-1} and 26,605 J mole^{-1} at 400°K ($4RT$ and $8RT$, respectively). Attention is drawn particularly to the behavior of $\bar{S}$ in the region of $x = 2$ due to the reduction in entropy on filling the lower energy level, followed, at slightly higher x, by an increase as the higher level becomes populated. The shape observed is very sensitive to the height of the energy level difference compared to RT, but is always symmetrical about $x = 2$.

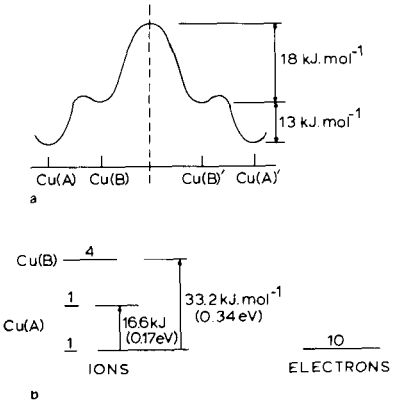

FIG. 3. (a) Possible energy profile along Cu ion conduction path. (b) Energy level model chosen for $Cu_xMo_6S_{7.59}$.

Interactions between Particles

In the treatment so far the limited number of sites available to the ions has been taken into account, but the ions themselves have been considered to be completely noninteracting. Although a thorough treatment of ion–ion interactions is complicated it is possible to deal with the case where the internal energy of an ion depends on the presence or otherwise of ions on equivalent sites within the same unit cell.

Consider an energy level n_j containing two equivalent sites per unit cell. To account for interaction it is necessary to divide it into two sublevels, n_{ja} and n_{jb}, each capable of containing one ion. Thus the first ion goes into n_{ja} and the second into n_{jb} with a different internal energy because of interaction with the ion in n_{ja}. The number of ions in n_{ja} is given as before by

$$n_{ja} = g_a/(1 + \exp(u_{ja} - \mu)/RT). \tag{10}$$

However, the situation for level n_{jb} is slightly different because the number of such sites available depends on the occupancy of n_{ja} (i.e., the number of n_{jb} sites is given by the number of *singly* occupied n_j sites); thus

$$n_{jb} = n_{ja}/(1 + \exp(u_{jb} - \mu)/RT). \tag{11}$$

In practice it was found that the differences in the calculated values of $\bar{S}$ and $\bar{U}$ using this approach compared with considering n_{jb} and n_{ja} as distinct energy levels not "sharing" the same sites is very small.

Thermodynamic Model for $Cu_xMo_6S_8$

Evidence Leading to Choice of Ionic Model

The structure of $Cu_xMo_6S_8$ has been discussed in the accompanying paper (*1*). There

are two sets of six equivalent copper ion sites per unit cell, denoted Cu(A) and Cu(B) sites. From X-ray occupancy measurements (*9*) and ionic conductivity (*1*) it was shown, however, that the maximum occupancy of the Cu(A) sites is about 1.8, presumably because of strong coulombic repulsion between the copper ions. The small distance between adjacent Cu(A) and Cu(B) sites also prevents these from being simultaneously occupied. Yvon thus concluded that a maximum total of six sites may be filled and we suggest that these are two Cu(A) and four Cu(B) sites. The variation in the activation energy for ionic conduction (*1*) indicates that the energy difference between Cu(A) and Cu(B) sites is about 13 kJ/mole, so that the energy profile over which a copper ion has to pass on going from one site cluster to another may be similar to that shown in Fig. 3. Cu(A)′ and Cu(B)′ are in a unit cell adjacent to Cu(A) and Cu(B).

More supporting evidence for this model comes from the partial thermodynamic quantities depicted by circles in Figs. 2, 5, and 6. The partial enthalpy shows a rapid increase of about 11 J mole^{-1} °K^{-1} in the region of $x = 2$ showing that the higher-energy sites begin to be filled at this composition. The change is in good agreement with that from the activation energy for ionic conduction. The partial entropy shows the same shape, centred on $x = 1.9$, as that observed for the model depicted in Fig. 4. Taking into account also the difference between the maximum and minimum in $\bar{S}$ it appears that an energy level is full at $x = 1.9$ and that the next level is higher by some $5RT$ to $6RT$.

The cell emf itself, which is proportional to the negative of the metal chemical potential, shows a small inflection at $x = 1.9$, and evidence of another around $x = 0.9$. The latter suggests that there may be quite a strong interaction between the two copper ions in A sites, which is not altogether surprising.

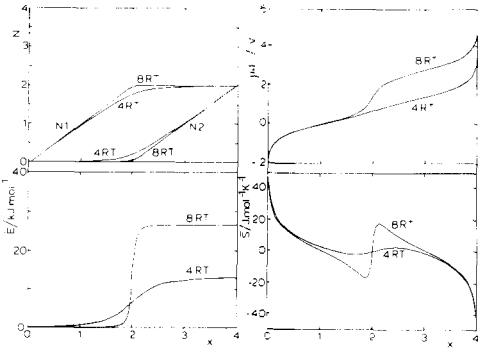

FIG. 4. Occupancy and partial quantities for models with particles distributed between two energy levels each with two equivalent sites. Results are shown for differences between the energy levels of $4RT$ and $8RT$.

Evidence Leading to Choice of Electronic Model

It is important to remember that we have so far ignored the contribution of the electrons to the partial quantities and attributed the observed changes entirely to the ions. $Cu_xMo_6S_8$ is a metallic conductor, but little is as yet known about the detailed band structure. The closely related lead compound, $PbMo_6S_8$ has, however, been the subject of two molecular orbital calculations (*10, 11*). These indicate some of the major features but differ in the precise positioning of the possible conduction bands relative to the Fermi level. The Fermi level probably lies within an Eg band capable of containing four electrons (*11*) but another six-electron Tg band lies nearby and may overlap this (*10*). In either case the conduction band becomes full when two further electrons are added, which is equivalent to the case of $Cu_4Mo_6S_8$. This upper limit to x corresponds to the ionic formula $Cu_4^{+}[Mo_6^{2+}S_8^{2-}]^{4-}$ as suggested by Yvon *et al.* (*9*). With our reduced sulfur content (*1*) this might be expected to lower the limit to $Cu_{3.4}[Mo_6^{2+}S_{7.7}^{2-}]$. From Fig. 1 it is seen that the actual limit must lie above $x = 3.5$, but whatever its exact value, the limit is imposed by the availability of electronic states, rather

than ionic sites. One can therefore expect a falloff in the electronic conductivity at x values near the limit. This is not so easy to test since the copper metal activity reaches unity at $x = 3.6$. Nevertheless, a decrease of about 15% in the electronic mobility as x increases from 2 to 13.2 has been reported (*12*). The width of the conduction band has been estimated to be around 0.6 eV or $17RT$ at 400°K, although the change in Fermi level over the range of occupancies corresponding to $1.5 < x < 3.5$ would only be a fraction of this. A significant electronic contribution to $\bar{H}$ is therefore quite possible.

Energy Level Model Chosen

The energy difference between Cu(A) sites (already containing one ion per unit cell) and Cu(B) sites was taken as $5RT$, a compromise between the indications discussed earlier. In the case of the electrons the next highest level above the conduction band is so large compared to RT that it could be ignored. The energy levels are shown in Fig. 3b and the resulting values of u_{Cu}, U, S, and N, calculated for 400°K, are shown by solid lines in Figs. 2, 5, 6, and 7, respectively.

Comparison of Model Calculations with Experimental Data

Occupancy of Copper Ion Sites

The data of Yvon *et al.* (*9*), presumably for ambient temperature, are compared to calculated occupancies in Fig. 7. There is insufficient experimental data for a thorough comparison to be made, but it appears that the main inadequacy of the model is that it does not explain the slight decrease in $N(A)$ at moderately high values of x. The fact that the maximum value of $N(A)$ is nonintegral suggests that either there is a long-range order operating due to interactions between copper ions in neighboring unit cells or that one is observing a time average of the positions of the copper ions as they move about thermally within the structure.

Partial Enthalpy

This is compared with experimental data in Fig. 5. The calculated line has been adjusted in the y direction to coincide with experiment at $x = 3.5$. Two regions deviating strongly from the calculated curve are apparent. At $x < 1.7$, $\bar{H}_{exp}$ decreases as x increases. This might tentatively be explained by the rapid changes in cell parameters that occur in this region (*13*). In particular the rhombohedral angle α increases with x and a consequent increase in the diameter of the group of Cu ion sites is expected, as explained by Yvon (*14*). This would lead to a decrease in the internal energy since the Cu^+ ions would on average move further apart. Below $x = 1$, however, a drop in H is visible, possibly due to the removal of Cu^+–Cu^+ ion repulsion when each unit cell contains at most only one ion.

In the region $2.2 < x < 2.5$ the lack of increase of $\bar{H}$ with x may be due also to the continuing, but smaller, rate of increase of α. At $x = 3$ the inflection may indicate the onset of further ion–ion repulsion on introduction of the second Cu ion in the B sites. There may

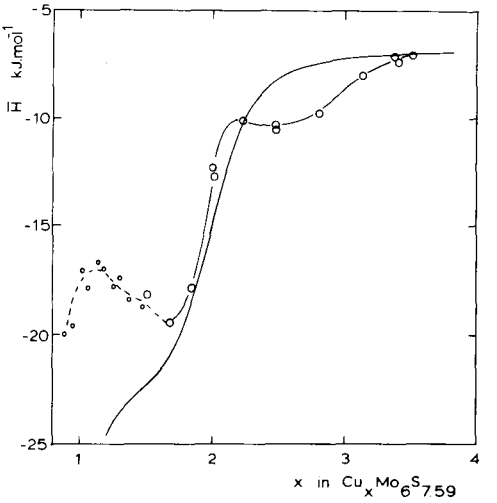

FIG. 5. Partial molar enthalpy of copper as a function of x at 400°K. Large open circles: bar experiment; small open circles: pellet experiment; solid line: theoretical model.

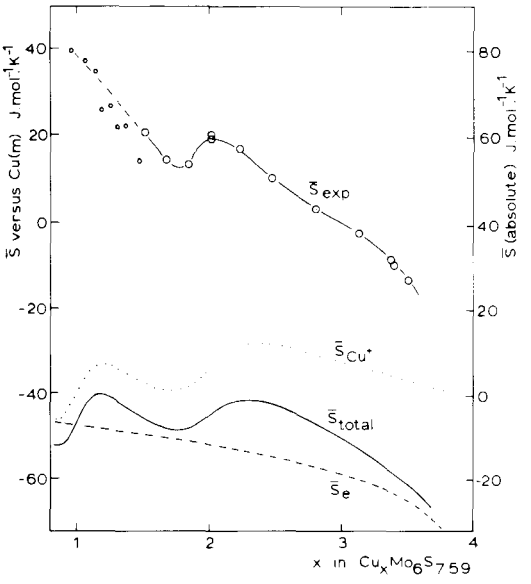

FIG. 6. Partial molar entropy of copper as a function of x at 400°K. Large open circles: bar experiment; small open circles: pellet experiment; dotted line: theoretical model, contribution from ions; dashed line: theoretical model, contribution from electrons; solid line: theoretical model, total.

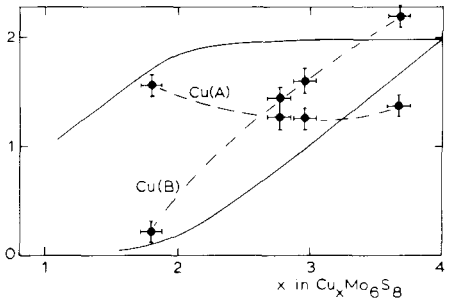

FIG. 7. Cu^+ site occupancies. Circles from Yvon *et al.* (*9*) at ambient temperature. Solid lines from theoretical model at 400°K.

also be a contribution to $\bar{H}$ from the electrons, due to finite width of the conduction band.

Partial Entropy

This is shown in Fig. 6. On the right-hand side is shown the absolute value of $\bar{S}$ obtained by adding the value of the absolute entropy of copper metal at 400°K, calculated from available data (*15*). Since the calculated values are absolute values of the configurational entropy it is thus possible to see the relative magnitude of the configurational entropy to other terms. It can be seen that these other terms, although large, are much less sensitive to x, so that the main features of the experimental curve are reproduced by consideration only of configurational terms. Perhaps the next most important contribution to $\bar{S}$ would arise from the low-frequency vibration modes associated with movement of copper ions within the groups of sites. This may explain the difference between the observed and calculated positions of the maximum in S in the region of $x = 2$.

Chemical Potential of Copper Metal

This is shown by the solid line in Fig. 2. Although the detailed shape is not well reproduced the overall variations with composition are correct.

Conclusions

Taking a very simple energy level model for the mobile species it has been possible to reproduce the main features of the partial enthalpy, entropy, and free energy of copper (atoms) in $Cu_xMo_6S_{7.59}$ as a function of x. We thus conclude that it is changes in configurational quantities which are responsible in the main for the variation of these quantities with composition. Other factors, although important, are not so composition dependent. This may be normally the case with solid solution electrode materials, since it has also been shown to be so for some of the layer compounds (*7*). If this is so it offers a relatively simple way to understand and perhaps predict the voltage composition behavior of other SSE materials. As has already been shown (*1*) the variations of the transport properties of $Cu_xMo_6S_{7.59}$ composition can also be explained in terms of a similar energy level model.

Appendix

It was shown earlier that the number of possible distinguishable arrangements of ions among the sites is

$$\Omega = \sum_l \prod_j (g_j!/[n_{jl}!(g_j - n_{jl})!]). \quad \text{(A1)}$$

For the very large numbers of ions involved however, it can be shown that only the biggest term in the summation, ω^*, containing n values corresponding to the most probable occupation of each of the sites, need be retained. Thus, taking logs:

$$\ln \omega = \sum_j [\ln g_i! - \ln n_j! - \ln(g_j - n_j)!]. \quad \text{(A2)}$$

Using Stirling's formula this approximates to

$$\ln \omega = \sum_j [g_j \ln g_i - n_j \ln n_j - (g_j - n_j) \ln (g_j - n_j)]. \quad \text{(A3)}$$

For this to be the largest term,

$$\delta \ln \omega_m = \sum_j [-\ln n_j + \ln(g_j - n_j)]\delta n_j = 0. \quad \text{(A4)}$$

Conservation of ions and total energy requires

$$\alpha \sum \delta n_j = 0, \qquad \beta \sum u_j \delta n_j = 0, \quad \text{(A5)}$$

and by the method of Lagrange's undetermined multipliers one obtains

$$\sum_j [-\ln n_j + \ln(g_j - n_j) - \alpha - \beta u_j]\delta_{n_j} = 0. \quad \text{(A6)}$$

Since the n_j values are independently variable, each term in brackets must separately be equal to zero. Hence,

$$\ln[(g_j - n_j^*)/n_j^*] - \alpha - \beta u_j = 0, \qquad \text{for all } j, \quad \text{(A7)}$$

and rearranging,

$$n_j^* = g_j/[\exp \alpha \cdot \exp(\beta u_j) + 1]. \quad \text{(A8)}$$

The entropy S is defined by $S = K \ln \Omega = K \ln \omega_m$. Thus,

$$S = K \sum_j [g_j \ln g_j - n_j^* \ln n_j^* - (g_j - n_j^*) \ln(g_j - n_j^*)]. \quad \text{(A9)}$$

Combining with Eq. (A8) one obtains

$$S = K \sum_j [-g_j \ln[1 - 1/(\exp \alpha \cdot \exp(\beta u_j) + 1)) + n_j^*(\alpha + \beta u_j)]. \quad \text{(A10)}$$

With $\sum n_j^* = N$ one obtains

$$S = kN\alpha + k\beta u + k \sum_j g_i \ln(1 + \exp \alpha \cdot \exp(-\beta u_i)). \quad \text{(A11)}$$

The thermodynamic relations $(dS/dU)_{N,V} = 1/T$ and $T(dS/dN)_{E,V} = \mu$ allow α and β to be identified:

$$\alpha = -\mu/kT, \qquad \beta = 1/kT. \quad \text{(A12)}$$

Hence one obtains Eq. (5).

Acknowledgments

We thank Mr. C. Stewart for performing some of the electrochemical measurements, and acknowledge financial support from the Anglo-Danish E.E.C. Project, Contract 316-78-EE.

References

1. G. J. DUDLEY, K. Y. CHEUNG, AND B. C. H. STEELE, *J. Solid State Chem.* **32**, 259 (1980).
2. B. C. H. STEELE, *in* "Superionic Conductors" (G. D. Mahan and W. L. Roth, Eds.), pp. 47–65, Plenum, New York (1976).
3. G. J. DUDLEY AND B. C. H. STEELE, *J. Solid State Chem.* **21**, 1 (1977).
4. W. WEPPNER AND R. A. HUGGINS, *J. Solid State Chem.* **22**, 297 (1977).
5. M. S. WHITTINGHAM, *Progr. Solid State Chem.* **12**, 1 (1978).
6. A. T. FROMHOLD, JR., "Theory of Metal Oxidation," Vol. 1, North-Holland, Amsterdam (1976).
7. M. ARMAND, Thesis, Grenoble (1978).
8. e.g., R. E. BARIEAU, *J. Chem. Phys.* **21**, 1827 (1953).

9. K. YVON, A. PAOLI, R. FLÜKIGER, AND R. CHEVREL, *Acta Crystallogr. B* **33**, 3066 (1977).
10. L. F. MATTHEIS AND C. Y. FONG, *Phys. Rev. B* **15**, 1760 (1977).
11. O. K. ANDERSEN, W. KLOSE, AND H. NOHL, *Phys. Rev. B* **17**, 1209 (1978).
12. R. FLUKIGER, A. JUNOD, R. BAILLIF, P. SPITZLI, A. TREYVAUD, A. PAOLI, H. DEVENTAY, AND J. MULLER, *Solid State Commun.* **23**, 699 (1977).
13. K. Y. CHEUNG AND B. C. H. STEELE, to be published.
14. K. YVON, *Solid State Commun.* **25**, 327 (1978).
15. R. C. WEST (Ed.), "Handbook of Chemistry and Physics," 55th ed., CRC Press, Cleveland, Ohio (1974).